

Modelling for Gas Transport in Enhanced Polymeric Blend Membrane

Asim Mushtaq*, Hilmi Mukhtar and Azmi Mohd Shariff
 Chemical Engineering Department, Universiti Teknologi PETRONAS,
 32610 Bandar Seri Iskandar, Perak, Malaysia.
 engrasimmushtaq@yahoo.com*

(Received on 19th June 2018, accepted in revised form 28th December 2018)

Summary: The main aim of this research work is to develop a model of carbon dioxide (CO₂) separation from natural gas by using membrane separation technology. This study includes the transport mechanism of the porous membrane. The fundamental theories of diffusion, poiseuille (viscous) flow, Knudsen diffusion and surface diffusion are used. The developed model of incorporating three diffusion mechanisms to be modified for modeling of polymeric blends towards membrane selectivity and permeability. For the purpose of assessing the gas permeance using the theoretical models, the experimental data taken from CO₂ permeance in the PSU/PVAc (85/15) wt. % /DEA enhanced polymeric blend membrane was considered. The results obtained from modified Cho Empirical model of total gas permeance showed the least error as compared to other models. The modified Cho Empirical mathematical models were extended by blending factor to predict CO₂ gas molecule transport in Enhanced Polymeric Blend Membrane (EPBM) to obtain precise theoretical values that are close to the experimental values. The Extended modified Cho Empirical model validation demonstrated the ability to predict CO₂ permeance with reasonable accuracy.

Keywords: Carbon dioxide; Methane; Polymeric blend membrane; Porous models; Permeance.

Introduction

Gas separation processes involve both upstream and downstream flows through the membrane. The pressure gradient occurs between these two streams facilitates separation. Permeation is the rate of gas diffuse across the membrane while the degree of separation depends on membrane selectivity under conditions of separation, which include temperature, pressure, flow rate and membrane area [1-3]. The transport of gasses across the membrane can be described using the following schematic diagram.

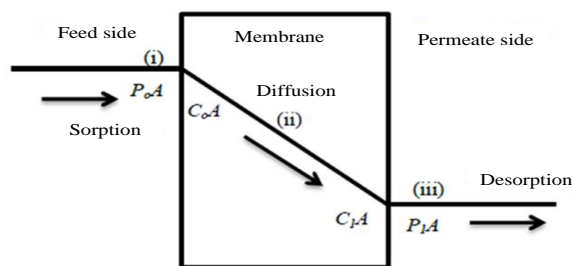


Fig. 1: Gas transport through membrane.

Fig 1 shows the two major processes sorption and diffusion that play main roles within the overall gas transport. Sorption defines the interactions between gas molecules and therefore the membrane surface, and diffusion refers to the rate of gas passage through the membrane [2, 4]. Quantitative and qualitative analysis of the

involvement of these steps is important so as to grasp the gas transport mechanism. As each process will contribute to the total permeation rate, and its importance can vary allowing to such variables as pressure, temperature, and composition. Sorption of gas molecules from the bulk gaseous state to the membrane surface can occur chemically or physically liable on the nature of the force between the surface and the gas molecules [5]. In the following transport process, the adsorbed molecules diffuse through the membrane in a very numerous manner beneath the driving forces such as concentration and pressure. The process reverses to sorption is known as desorption. This occurs in a system being in the state of sorption equilibrium among an adsorbing surface and bulk phase. Once the pressure or concentration of the substance in the bulk phase is lowered, some of the sorbed substance modified to the bulk state [6].

Table-1: Gas permeability and permeance units.

Expression	Unit	Dimension
Permeability, P_A	Barrer	10^{-10}
		$\frac{\text{cm}^3(\text{STP}) \cdot \text{cm}}{\text{cm}^2 \cdot \text{sec} \cdot \text{cmHg}}$
Permeance, $\frac{P_A}{l}$	Gas Permeation Unit (GPU)	10^{-6}
		$\frac{\text{cm}^3(\text{STP})}{\text{cm}^2 \cdot \text{sec} \cdot \text{cmHg}}$

The units of permeability and permeance across the membrane are given in Table-1 [7]. Generally, membranes models can be divided into

*To whom all correspondence should be addressed.

two categories according to their structural characteristics, dense and porous membranes. The dense membranes are free of discrete structure. The difference between the dense and porous can be conveniently detected by the presence of any pore structure beneath electron microscopy. The efficiency of a membrane strongly depends on the selection of material used, the type of species to be separated and their interactions of species gases with the membrane [8].

Theory

Gas Transport Mechanism in Porous Membrane

The properties of gas flow in porous media can be determined by the ratio of molecule-molecule collisions and the molecule-wall collisions as shown in Fig. 2.

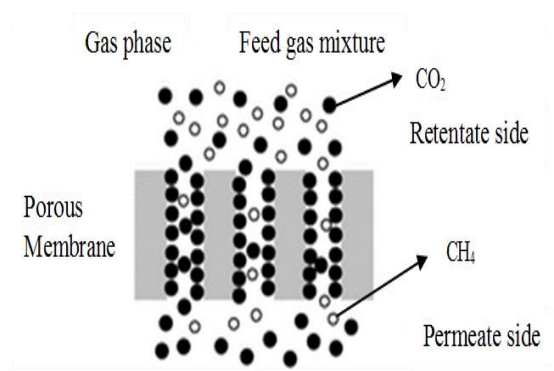


Fig. 2: Gas transport in porous membrane.

The membrane dependent on membrane pore size and the sizes of the pore depending the process gasses. The pores characteristics of porous materials have a very complex structure and morphology and many studies have been devoted to describing and characterizing them [6, 8]. Schematic diagram of different types of pores is given in Fig. 3. As can be seen in the diagram, isolated pores, and dead ends do not contribute to the permeation in steady conditions. Dead ends do also subsidize to the porosity as measured by adsorption techniques but do not contribute to the actual porosity in permeation [9]. Pore shapes are channel - like or slit - shaped. Pore constrictions are significant for flow resistance, particularly when surface diffusion and capillary condensation phenomena occur in systems with a quite large internal surface area.

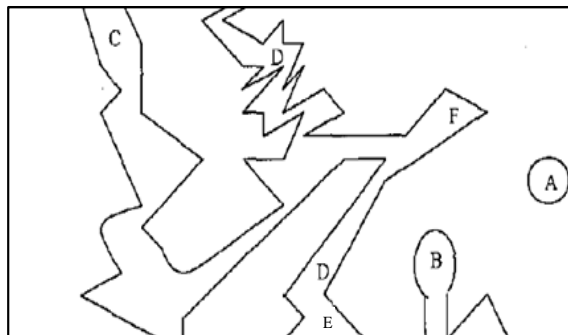


Fig. 3: Schematic diagram of different types of pores in a porous solid. A: Isolated pore; B, F: dead end pores; C, D: Tortuous rough pores; E: Conical pore.

The four basic transport mechanisms across porous membranes are known as Poiseuille flow, Knudsen diffusion, surface diffusion and capillary condensation [7, 11]. For effective separation a mixture of chemical components, a membrane must have a high permeance and its ratio for the species enduring separation [7]. Permeance for a certain species diffusing through a membrane of a known thickness is closely resembling a mass transfer coefficient for the flow rate of that species per unit of cross-sectional area of membrane per unit of driving force [7]. The molar trans-membrane flux of a species i is given by;

$$N_i = \frac{P'_i}{t_m} f_d \quad (1)$$

where P'_i is the permeability of gas species i , f_d is driving force and t_m is membrane thickness. When a mixture on each side of a microporous membrane is gas, Fick's law expresses the rate of a species diffusion. When pressure and temperature on either side of the membrane are equal, and the ideal gas law holds, the trans-membrane flux is expressed in terms of a partial pressure driving force as follows [7]:

$$N_i = \frac{D_{e,i} C_m}{P t_m} (p_{i,o} - p_{i,L}) \quad (2)$$

where C_m is the total concentration of the gas mixture given as P/RT by the ideal gas law. Thus, equation (2) can be written otherwise as [7]:

$$N_i = \frac{D_{e,i}}{RT t_m} (p_{i,o} - p_{i,L}) \quad (3)$$

The detail description of the four basic transport mechanism is discussed in the following section.

Poiseuille flow

Viscous (Poiseuille) flow plays an important role in the macroporous substrate(s) supporting the separation layer and can affect the total flow resistance of the membrane system. Gas flow takes place by normal convective flow i.e. $r/\lambda > 1$ if the pores of a microporous membrane are 0.1 microns or larger [12]. The Poiseuille flow is also known as viscous flow. The assumption that the pore resembles a perfect cylinder is necessary to model the viscous flow in the pore [11]. This assumption is practical for a piece of thin membrane with a pore size from 1-7 nm, as the gas molecules will collide more frequently with each other than their collision through the cylinder wall, under this condition [13]. Fig 4 show the viscous diffusion.

$$J = \frac{\Delta P \epsilon d_p^2}{32 \tau \mu l} \quad (4)$$

where J is the flux, l is the pore length, d_p is the pore diameter, ΔP is the pressure difference across pore, μ is the solvent viscosity, ϵ is the porosity ($\pi d_p^2 N/4$, where N is number of pores per cm^2), typical pore diameter: MF – 1micron; UF – 0.01 micron.

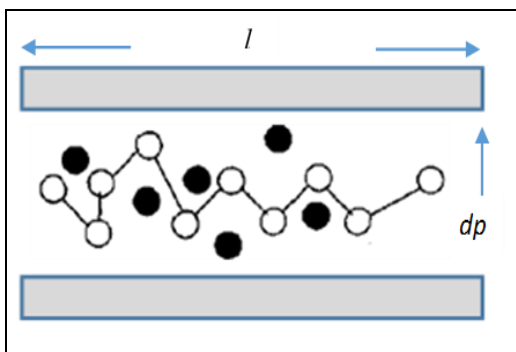


Fig. 4: Viscous diffusion across membrane.

The average velocity, v_{av} of gas molecule is defined as:

$$v_{av} = \frac{1}{2} \left[\frac{p_h - p_l}{4 \mu_i t} \right] r_p^2 \quad (5)$$

where p_h is the high pressure, p_l is a low pressure, μ_i is the viscosity of gas i , t is the time and r_p are the radius of the pore.

For total volumetric flow rate across the whole piece of membrane, the number of pores q_p can be calculated as,

$$\text{Number of Pore} = \epsilon \left(\frac{\text{Membrane area}}{\text{Cross sectional area of pore}} \right) \quad (6)$$

$$\text{Number of Pores} = \frac{2 \epsilon R_m L_m}{r_p^2} \quad (7)$$

where L_m is the length of the cylindrical pore and R_m is the radius of the cylindrical pore

$$q_p = \frac{\epsilon \pi R_m L_m r_p^2}{4 \mu_i t} (p_h - p_l) \quad (8)$$

The value of gas permeability can also be determined experimentally as was done by Lee and Hwang in 1985 [14];

$$P'_i = \frac{q_p t_m}{A_m \Delta P} \quad (9)$$

From equation (8) and (9), the permeability of gas molecule through the membrane pores, due to viscous diffusion, can thus be calculated as such:

$$P'_i = \frac{\epsilon r_p^2}{8 \tau \mu_i} \quad (10)$$

Equation (10) shows that the permeability of gas molecule does not depend on the pressure of the system. It is only a function of the membrane pore size, tortuosity, porosity and the viscosity of the gas. It is important to note that the permeability of gas is a function of temperature indirectly, as the viscosity of gas varies with system temperature. The viscosity of gas can be computed by using the empirical correlation as established by Bird et al. [15]:

$$\mu = 2.6693 \times 10^{-5} \frac{\sqrt{M_i T}}{\sigma_i^2 \Omega_{i,\mu}} \quad (11)$$

Knudsen Diffusion

Mesoporous separation layers are commonly in the transient – regime among Knudsen diffusion and molecular diffusion, with large effects on the selectivity (separation factor). Convective flow will be replaced by Knudsen diffusion in a porous membrane, whose pore sizes are less than the mean free path of the gas molecules [16]. Knudsen diffusion arises when the ratio of the pore radius to the mean free path ($\lambda \sim 0.1$ microns) of a gas molecule is less than 1. Diffusing gas molecules then

have further collisions with the pore walls and other gas molecules as shown in Fig 5. Gases with high D_K permeate preferentially [12].

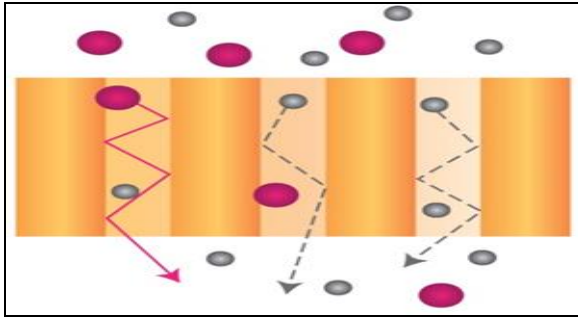


Fig. 5: Knudsen diffusion mechanism.

For an equimolar feed, the permeation rate of Knudsen diffusion is inversely proportional to the square root of the molecular weight of the different compounds in the following equation [17]:

$$D_K = 0.667rv = 97r_p \sqrt{\frac{T}{M_w}} \quad (12)$$

where D_K (m^2/s) is the Knudsen diffusion coefficient, r_p is the average pore radius, v is the average molecular velocity (m/s) and T is the operating temperature.

According to Seader and Henley [7], the ordinary and Knudsen diffusions, D_i and $D_{k,i}$ of gas species i can be estimated using equation (13) and (15), respectively written as:

$$D_i = \frac{0.86}{P} \quad (13)$$

Gas diffusion through a pore occurs by ordinary diffusion and/or in series via Knudsen diffusion when the pore diameter is very small and/or total pressure is low. In the Knudsen-flow regime, more collisions occur between gas molecules and the pore wall than between gas molecules. In the absence of bulk-flow effect or restrictive diffusion, equation (14) is modified to account for both mechanisms of diffusions:

$$D_{e_i} = \frac{\varepsilon}{\tau} \left[\frac{1}{\left(\frac{1}{D_i}\right) + \left(\frac{1}{D_{K_i}}\right)} \right] \quad (14)$$

where D_{e_i} is the effective diffusivity, D_{K_i} is the Knudsen diffusivity, which from the kinetic theory of

gases as applied to a straight, cylindrical pore of diameter d_p is

$$D_{K_i} = \frac{d_p \bar{v}_i}{3} \quad (15)$$

where \bar{v}_i is the average molecule velocity given by [10]:

$$\bar{v}_i = \left(\frac{8RT}{\pi M_i} \right)^{\frac{1}{2}} \quad (16)$$

where M is molecular weight. Combining equation (15) and (16):

$$D_{K_i} = 4850 d_p \left(\frac{T}{M_i} \right)^{\frac{1}{2}} \quad (17)$$

where D_K is cm^2/s , d_p is cm and T are K.

By integrating the equation (1), (3) and (14), the final equation to calculate the permeability of gas species i through the membrane due to Knudsen and ordinary diffusions can be expressed as [7]:

$$P'_{\kappa,i} = \frac{\varepsilon}{RT\tau} \left[\frac{1}{\left(\frac{1}{D_i}\right) + \left(\frac{1}{D_{K_i}}\right)} \right] \quad (18)$$

Surface Diffusion

When the temperature of the gas is such that adsorption on pore walls is important, experimental results illustrate that the previous laws for gaseous flow are no longer effective [10].

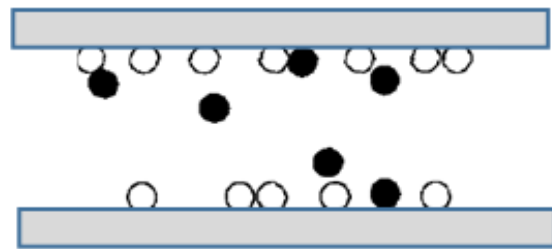


Fig. 6: Surface diffusion mechanism.

For comparatively low surface concentrations, the surface flux, J_s , for a single gas is generally described by the two-dimensional Fick's law [10]:

$$J_s = -2 \frac{t_m \epsilon^2}{r_p \tau} (1 - \epsilon) D_s \frac{dC_s}{dZ} \quad (19)$$

The surface concentration, C_s , can be correlated with the membrane density ρ_m , and the uptake of the gas molecules by the sorbent material h , which has the unit of [mol.g⁻¹] by the following equation [18].

$$C_s = \rho_m h \quad (20)$$

By inserting equation (20) into equation (19) yields

$$J_s = -2 \frac{t_m \epsilon^2}{r_p \tau} (1 - \epsilon) D_s \rho_m \frac{dh}{dZ} \quad (21)$$

The uptake of the gas species by the sorbent material, h , is approximated by Henry's law (monolayer adsorption is assumed to take place) to be directly proportional to the equilibrium loading factor, f , and system pressure as below:

$$h \propto fP \quad (22)$$

Dimensional analysis of equation (22) yields;

$$h = \frac{1}{zRT} (fP) \quad (23)$$

Keizer et al. showed that f is directly proportional to pressure and inversely proportional to temperature [19]. By inserting h from equation (22) into equation (21) yields:

$$J_s = -2 \frac{r_p \epsilon^2}{t_m \tau} (1 - \epsilon) \frac{D_s \rho_m f dP}{zRT dZ} \quad (24)$$

where D_s , can be computed from the following empirical relation as established by Bird et al.:

$$D_s = 1.6 \times 10^{-2} e^{\left[\frac{0.45(-\Delta H)}{mRT} \right]} \quad (25)$$

where m is 2 for conductive sorbent and 1 for non-conductive sorbent and ΔH is the specific enthalpy [7]. The heat of adsorption of the gas species to the sorbent material can be approximated with the assumption that condensation occurs on the surface. It can be estimated by using Trouton's law and Watson Correlation [20].

With gas mixtures, enhancement of the separation factor can be obtained by preferential sorption of mobile species of one of the components of the gas mixture. Adsorption does not always lead to enhanced separation. In a mixture of light non-adsorbing molecules and heavy molecules, the heavy molecules move slower than the lighter ones but in many cases are preferentially adsorbed. Consequently, the flux of the heavier molecules is better enhanced by surface diffusion and the separation factor increases.

Pore distribution of the membrane material is normally not uniform and the pores can have very different shape, orientation, and length from each other. Thus, the diffusion of gas molecules through all the pores in a membrane system may not be necessary uniform or successful. Effective diffusion, D_e , is introduced to cater for this discrepancy between pores, and it can be obtained from Fick's Law as [7]:

$$J_T = -D_e \frac{dC}{dZ} \quad (26)$$

J_T the total flux that comprises the flux via gas diffusion and surface diffusion.

Substitution of $C = \frac{P}{zRT}$ into equation (26) yields,

$$J_T = \frac{-D_e dP}{zRT dZ} \quad (27)$$

From the true definition of J_T , the total flux can be written as,

$$J_T = J_g + J_s$$

$$J_T = -\frac{\epsilon}{zRT} \left(\frac{1}{D_i} + \frac{1}{D_{k,i}} \right) \frac{dP}{dZ} - 2 \frac{t_m \epsilon^2}{r_p \tau} (1 - \epsilon) \frac{D_s \rho_m f dP}{zRT dZ} \quad (28)$$

By equating equation (28) to equation (26), D_e is obtained as such,

$$D_e = \epsilon \left(\frac{1}{\frac{1}{D_i} + \frac{1}{D_{k,i}}} \right) + 2 \frac{t_m \epsilon^2}{r_p \tau} (1 - \epsilon) D_s \rho_m f \quad (29)$$

Gas Permeation Models for Porous Membrane

Permeability is a significant parameter in membrane performance. It gives an overview of permeation behavior of a certain gas through a

specific type of membrane, either less permeable or highly permeable. The measurement of gas permeability is usually done on pure gas species. The following literature will illuminate and discuss some of the gas permeability models developed by numerous researchers. The permeability, P'_i for a pure gas i can be measured from the Seader and Henley 1998 equation (18) [7].

Cho et al. 1995 developed an empirical model for gas permeability prediction based on the three important transport mechanisms in the membrane, namely viscous flow, Knudsen diffusion and surface diffusion [21]. The model is shown as follows:

$$P'_i = \frac{\varepsilon \eta r_p^2}{8\mu_i RT} \bar{P} + \frac{2\varepsilon \eta r_p}{3RTL} \left(\frac{8RT}{\pi M_i} \right)^{\frac{1}{2}} + \frac{2\varepsilon \eta D_s}{r_p AN_{av}} \frac{db_s}{dp} \quad (30)$$

The first term in the above equation represents the viscous flow. The second term caters for Knudsen diffusion whereas the third term describes the surface diffusion that occurs in the pores. It was illustrious that the second term is not dimensional homogeneous with the first and third term [21]. It should not contain the thickness of the membrane in the equation. Equation (30) has been improved from this error so that it is dimensional homogeneous. The error in the relation as developed when the pore size is so small that it approximates the size of a gas molecule, the effect due to pore refining is not obvious [21]. Moreover, Knudsen diffusion will not occur when the pore size is smaller than the size of the gas molecule. The value of gas permeability can also be determined experimentally as was done by Lee and Hwang in 1985 [14]. It was shown that the gas permeability can be described by the following relation as shown in equation (9).

From equation (9), it is apparent that permeability of the gas through the membrane will increase with respect to rising in q_p , if the other parameters stay the same. This is true, as more gas permeates through the membrane surface. However, the permeability of gas should increase, by right, when the thickness of membrane decreases and not the other way around as suggested by equation (9). This is because the distant of travel of the gas molecules will decrease as the thickness reduces and thus the gas molecules need the least time to complete the whole path. But, do not neglect the fact that the actual lengths of travel, t of the gas molecules are generally much longer than the membrane thickness, t_m , due to the intrinsic structure of the pores. As seen from equation (18), the permeability

of gas is inversely proportional to the tortuosity of the membrane material, which is a ratio of t to t_m [7, 22]. Hence, it can be concluded that equation (10) is actually true, as the increase of t_m will result in a less tortuous membrane material and consequently shows an increase in permeability.

In the Dusty Gas Model (DGM) as presented by Mason and Malinaukas, all the different contributions to the transport are taken into account [9]. According to the model assumption, the wall of the porous medium is considered as a very heavy component and so contributes to the momentum transfer. The model is schematically represented in Fig 7 for a binary mixture. As can be seen from this electrical network analogy, the flux contributions by Knudsen diffusion $J_{k,i}$ and molecular diffusion of the mixture $J_{m,12}$ are in series and so are coupled. The total flux of component i ($i=1,2$) due to these contributions is $J_{i,km}$. The contribution of the viscous flow $J_{v,i}$ and of the surface diffusion $J_{s,i}$ are parallel with $J_{i,km}$ and so are considered independent of each other. There is no transport interaction between gas phase and surface diffusion. The flux expression for single species i in a multi - component mixture with n components according to the DGM model results in [10].

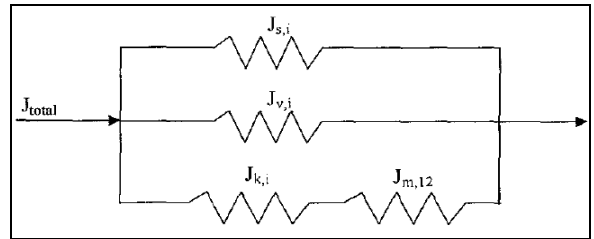


Fig. 7: Dusty gas model.

$$\sum_{j=1, j \neq i}^n \frac{x_i \cdot J_j - x_j \cdot J_i}{P_i D_{ij}^e} - \frac{J_i}{P D_{i,k}^e} = \frac{1}{RT} \frac{\delta x_i}{\delta z} + \frac{x_i}{PRT} \left(\frac{B_o P}{\eta D_{i,k}^e} + 1 \right) \frac{\delta P}{\delta z} \quad (31)$$

$$D_{i,k}^e = \frac{\varepsilon A}{\tau^3} K_n \sqrt{\frac{8RT}{\pi M_i}}$$

where K_n as the Knudsen number.

$$D_{i,k}^e = 0.00262 \sqrt{\frac{T^3 \left[\frac{M_1 + M_2}{2M_1 M_2} \right]}{P \sigma_{12}^2 \Omega_{12}}}$$

Present and De Bethune was the first to develop a model (P - D model) including diffusion, intermolecular momentum transfer, and viscous flow

[23]. Based on the P-D model, Eickmann and Werner incorporated two parameters (n_k and β) in the P - D equations to account for geometric and reflection characteristics of a real membrane [17]. This extended P - D model is very successful to describe the effect of parameters on permeation and separation. Note that surface diffusion is not incorporated in the model. The flux of component i in a binary mixture is given by:

$$J_i = \frac{g'}{L} \left[\frac{\alpha_o}{1+B'P} \frac{d(x.P)}{dz} + \frac{f_o B' x P}{1+B'P} \frac{dP}{dz} + x A' P \frac{dP}{dz} \right] \quad (32)$$

The mole fractions for components 1 and 2 ($i = 1, 2$) given by x and $1-x$, respectively. The first term in equation (32) describes the Knudsen diffusion while the second and third term accounts for momentum transfer and viscous flow respectively. The different coefficients in equation (32) can be obtained from Burggraaf and Cot [10].

Modeling in Polymeric Membrane

The permeability of gas molecule in porous material as combined influences by all the three types of transport mechanism such as viscous, Knudsen, and surface diffusion [24]. The total permeability of gas species i , P'_i could be obtained by summation of all the three mechanisms permeability.

The trans- membrane flux of a gas species, N , can be related as follow,

$$N = \frac{P'_i}{t_m} (p_h - p_l) \quad (33)$$

By equating equation (33) with equation (27), which is $N = J_T$,

$$\therefore P'_i = \frac{D_e}{z\tau RT} (p_h - p_l) \frac{t_m}{(p_h - p_l)} \quad (34)$$

Knowing that $\tau = \frac{t}{t_m}$, hence,

$$P'_i = \frac{D_e}{z\tau RT} \quad (35)$$

By substituting the relation for D_e , from equation (29) into the above equation,

$$P'_i = \frac{\mathcal{E}}{z\tau RT} \left(\frac{1}{\frac{1}{D_i} + \frac{1}{D_{k,i}}} + 2 \frac{t_m \mathcal{E}}{r_p \tau} (1 - \mathcal{E}) D_s \rho_m f \right) \quad (36)$$

Permeability of gas as the result of viscous diffusion, as shown in equation (10) can be unified with equation (36) to model the characteristic model of gas permeability as a function of the three important mechanisms of transport in pores,

$$P'_i = \frac{\mathcal{E} r_p^2}{8\tau \mu_i} + \frac{\mathcal{E}}{z\tau RT} \left[\left(\frac{1}{\frac{1}{D_i} + \frac{1}{D_{k,i}}} \right) + 2 \frac{t_m \mathcal{E}}{r_p \tau} (1 - \mathcal{E}) D_s \rho_m f \right] \quad (37)$$

Dimensional analysis of the above equation shows that term 1 [$\text{m}^3 \cdot \text{s} \cdot \text{kg}^{-1}$] is not dimensional homogeneous with term 2 and 3 [$\text{mol} \cdot \text{s} \cdot \text{kg}^{-1}$]. The introduction of ideal gas law into term 1 will yield a dimensional homogeneous equation for gas permeability. From ideal gas law,

$$\frac{n}{V} = \frac{P}{zRT} \quad (38)$$

Substitution of equation (38) into equation (37),

$$P'_i = \frac{\mathcal{E}}{z\tau RT} \left[\frac{r_p^2 P}{8\mu_i} + \left[\left(\frac{1}{\frac{1}{D_i} + \frac{1}{D_{k,i}}} \right) + 2 \frac{t_m \mathcal{E}}{r_p \tau} (1 - \mathcal{E}) \right] [(D)_s \rho_m f] \right] \quad (39)$$

It is important to note that the pressure as mentioned in equation (39) is the pressure in the membrane pores. However, the measurement of pressure in the pores will be cumbersome and impractical. Thus, the pressure in the pores can be approximated as the average pressure between the feed and permeate side [18]. The contribution of viscous flow towards the permeability of gas is directly proportional to the average pressure between feed and permeate side. It may lose its entire effect towards permeability at high temperature as the gas viscosity is a strong function of temperature. However, for small and fine pores, the contribution of surface diffusion is more apparent.

P'_i represent the total permeability of gas i , \mathcal{E} is membrane porosity, r_p is pore size, τ is tortuosity, μ_i is the viscosity of gas i , z is compressibility factor of gas i depending on pressure, t_m is membrane thickness, ρ_m is membrane density and f is equilibrium loading factor. Meanwhile, R in equation (39) above stand for the universal gas constant which is equal to $82.06 \text{ cm}^3 \cdot \text{atm} / \text{mol} \cdot \text{K}$, P is the operating pressure and T is the

operating temperature. D_i and $D_{k,i}$ signify the ordinary and Knudsen diffusion of gas i while D_s is surface diffusion. From the equation above, the membrane properties like porosity (\mathcal{E}), density (ρ_m), tortuosity (τ) and membrane thickness (t_m) influence the permeability of gas species i together with operating pressure, P and temperature, T .

The first part of the equation (39) above characterizes the permeability of gas species due to viscous diffusion. The viscosity of a pure monatomic gas of molecular weight M_i using the Lennard-Jones parameters σ and Ω . The gas viscosity, μ is carrying the unit of g/cm.s provided the unit of T in Kelvin and σ in m (10^{-10} m). The dimensionless quantity Ω_μ is a slowly variable function of the dimensionless temperature KT/\mathcal{E} on the order of magnitude of unity. This accounts for details of the molecular paths taken during a binary collision and is called the collision integral for viscosity. Ω_μ is exactly unity if gasses comprise rigid spheres as an alternative of molecules with attractive and repulsive forces. Hence, this function (Ω_μ) can be interpreted as the deviation from rigid-sphere behavior. Although equation (2) is kinetic theory result of monatomic gasses, it remarkably fits polyatomic gasses as well [14, 25]. The second part of the right-hand side of equation (36) estimates the permeability of gas species i due to ordinary and Knudsen diffusion.

The permeability of gas species i due to the surface diffusion is represented by third part of the equation (39). Surface diffusion will only occur at small pore regions, but it gives the highest selectivity due to membrane material's preferential sorptivity of certain gasses than the others. The surface diffusion, $D_{s,i}$ for gas species i , could be obtained by using equation (25) as proposed by Seader and Henley [7]. For conducting adsorbent such as carbon, m is equal to 2 and for insulating adsorbents, m equal to 1 is used. Typically, the values of surface diffusivity of light gasses for physical adsorption are in the range of 5×10^{-3} to 10^{-6} cm²/s. In the case of a low differential heat of adsorption, larger values of D_s are applied.

In order to find out the efficiency of the membrane in separating the desired gas, an ideal separation factor, α (also known as selectivity) is calculated. The selectivity as the quotient of the permeability of two different gasses given as follow [26].

$$\alpha_{ij} = \frac{P'_i}{P'_j} \quad (40)$$

The term of α_{ij} is representing the selectivity of gas species i to gas species j while P'_i and P'_j are the permeability of gas species i and j , accordingly. The higher the value of α_{ij} means the better separation through that particular membrane has occurred.

Results and Discussion

The transport properties of PSU/PVAc blend membranes comprising an amount of amine have been examined and correlated with the morphological structure of the blend system. The porous structure by FESEM evidence, PVAc and amine are dispersed in a PSU matrix, also confirms its compatibility to form miscible blend mixtures.

Gas Transport in Enhanced Polymeric Blend Membrane (EPBM)

The development of enhanced polymeric blend membrane exhibited the good separation factor α (CO₂/CH₄) were in the range of 11.16 (base PSU membrane) to 31.30 (PSU/PVAc (95/5) wt. % /DEA) at 10 bar pressure [27]. Therefore, the enhancement in the performance of EPBM was due to the presence of the combined effect of polyvinyl acetate (rubbery polymer) and amine, in which the later attracts more solubility of CO₂ and retards the solubility of CH₄. The formation of complex mechanism can be better understood by modeling the transport of these gases using appropriate model. The transport mechanisms of these gases across these EPBM can be described as the viscous, Knudsen and surface diffusion.

The transport properties of PSU/PVAc blend membranes containing an amount of amine have been investigated and correlated with the morphological structure of the blend system. The porous structure by FESEM evidence, PVAc and amine are dispersed in a PSU matrix, also confirms its compatibility to form miscible blend mixtures [28]. The different composition of PVAc and amines were blended in PSU, change its pore diameter which effected the permeance rate according to the pressure [27]. Diffusion in PSU polymeric membrane is completely different from PVAc polymer membrane because of the difference in the characteristic scales of the micromotions that occur at a segmental level for the two states. In PSU polymeric membrane the motion of gas molecules is much less broad than PVAc polymeric membrane. It is known that the diffusion coefficient is the primary factor in determining the absolute value of gas permeability in polymers [29]. The diffusivity of gases was shown to decrease promptly as the collision diameter of the gas molecule

increases. The diffusion coefficient changed ten orders of magnitude with an order of magnitude change in diameter [18]. Other molecular size parameters proposed include square root of molecular weight, molar volume, and Lennard-Jones or kinetic diameter [24]. The interactional relationship of these quantities gives distinctive results.

For the PSU membrane, surface diffusion is the dominant contributor to the total permeance of CO₂ at small pores and it decreases with increasing pore size [30]. Gas transport through PVAc is based on the differences in adsorption kinetics of different gases present in the gaseous mixture. In the separation of CO₂ and CH₄ by PVAc, smaller (3.3°A) CO₂ molecule adsorb more rapidly as compared to larger (3.8°A) CH₄ molecule. For amine EPBM, the type of amines is important for the high rate of diffusion. For CO₂ and CH₄ separation by di-ethanolamine (DEA), the diffusion rate of CO₂ is higher as compared to CH₄ due to the high affinity of CO₂ with DEA.

For the blend membranes PSU/PVAc/amines, at small pore sizes, the movement of the gas molecules are impeded by the narrow pathways of travel. Under this state, the gas molecules have higher tendency to diffuse from the bulk stagnant gas film to the pore surface due to the concentration gradient between bulk gas phase and pore surface. At the pore surface, adsorption of highly adsorbing CO₂ gas molecules takes place and thus, contributes to the high total permeability of CO₂. Due to the hindered pathways of travel, viscous diffusion and Knudsen diffusion are not apparent at very small pore sizes (<2 nm) [10]. A porous membrane, higher permeability indicates that the membrane has high porosity [2]. With reference to section 2.1 to 2.3, several models were discussed for the prediction of permeability of EPBM as Modified Cho empirical model, Cho empirical model, Lee and Hwang model, Seader and Henley model and other models [7, 10, 14, 21, 31]. The performance analysis of three existing models was carried out in section 3.2 to select the best working model for the prediction of enhanced polymeric blend membranes (EPBM).

Gas Permeance Analysis Using Modeling Approach in EPBM

When evaluating gas permeance using theoretical models, the experimental data was used from CO₂ permeance in the base PSU, PSU/PVAc and PSU/PVAc/DEA blends membranes. The principal mechanisms of gas permeation in porous material consist of viscous diffusion, Knudsen diffusion and surface diffusion. Along the simulation of the models, it was assumed that the surface diffusion, which

comprises the adsorption of gas molecules on the surface of the pores and then glides along the pores upon the pressure gradient, would behave as ideally as predicted by Henry's law [18, 24]. The basic models for gas permeation of porous polymeric membrane are given above. Basically, three models have been used for the performance analysis of current synthesized polymeric membrane which includes modified Cho empirical model (Eq. 39), Cho empirical model (Eq. 30), and Lee and Hwang model (Eq. 10). These models are basically developed from transport phenomena including viscous, Knudsen and surface diffusion. Despite their practicality and advantages, these models have been evaluated to have some limitations as stated below.

The Lee and Hwang model in 1985 proposed the viscous (Poiseuille) flow of gas permeability. The permeability of gas molecule does not depend on the pressure of the system as shown in equation (10). It is only a function of the membrane porosity, pore size, tortuosity and the viscosity of the gas [14]. According to Seader and Henley model (1998), gas diffusion through a pore occurs by ordinary diffusion or Knudsen diffusion only when the pore diameter is very small and total pressure is low as shown in equation (18) [7]. Cho et al. 1995 developed an empirical model for gas permeability. It was illustrious that the second term is not dimensional homogeneous with the first and third term. It should not contain the thickness of the membrane in the equation (30) [21].

Modified Cho empirical model (2004) stated that, the permeability of gas molecule in porous material as combined influences by all the three types of transport mechanism such as viscous diffusion, Knudsen diffusion and surface diffusion [31-33]. The total permeability of gas species could be obtained by summation of all the three mechanisms permeability. It is important to note that the pressure as mentioned in equation (39) is the pressure in the membrane pores. However, the measurement of pressure in the pores will be cumbersome and impractical. Thus, the pressure in the pores can be approximated as the average pressure between the feed and permeate side.

To assess the gas permeance using the theoretical model, the experimental data are taken from CO₂ permeance in the base PSU polymeric membrane, PSU/PVAc polymeric blend membranes and PSU/PVAc/DEA enhanced polymeric blend membranes was considered. The AARE% values were calculated by the following equation [34];

$$AARE\% = \frac{100}{n} \sum_{i=1}^n \left| \frac{P_i^{cal} - P_i^{exp}}{P_i^{exp}} \right| \quad (40)$$

Evaluation of Existing Models using Base PSU Membrane

Fig 8 shows the comparison between the existing models and the experimental data for base PSU membrane. It was found that the modified Cho empirical model is closest to the experimental results as compared to other models.

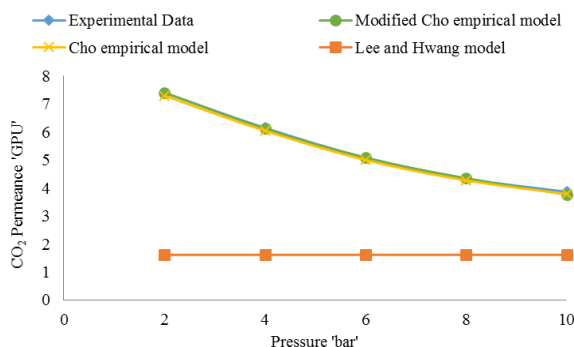


Fig. 8: Comparison of different models with experimental results for CO₂ permeance of base PSU membrane.

Table-2: Variation of the different existing models with the experimental data for CO₂ permeance of base PSU membrane

Theoretical models	Average Absolute Relative Error (AARE %) of base PSU membrane
Modified Cho empirical model (2004) Eq. 39	0.66
Cho empirical model (1995) Eq. 30	1.65
Lee and Hwang model (1985) Eq. 10	68.16

Table-2 shows the average absolute relative error (AARE%) between the CO₂ experimental and calculated permeance determined by different models for base PSU membrane. Lee and Hwang model has a greater error as compared to modified Cho empirical model and Cho empirical model. This is due to Lee and Hwang model only shows viscous flow of gas permeability. However, in modified Cho empirical and Cho empirical model, the gas permeance occurs in three phenomena's viscous, Knudsen and surface diffusion. From the table it was found that the modified Cho empirical model of base PSU

Table-3: Variation of the different existing models with the experimental data for CO₂ permeance of polymeric blend membranes

Theoretical models	Average Absolute Relative Error (AARE %) of polymeric blend membranes				
	Base PSU	PSU/PVAc (95/5) wt. %	PSU/PVAc (90/10) wt. %	PSU/PVAc (85/15) wt. %	PSU/PVAc (80/20) wt. %
Modified Cho empirical model (2004) Eq. 39	0.66	36.17	43.56	46.46	48.92
Cho Empirical model (1995) Eq. 30	1.65	39.25	41.63	50.20	55.95
Lee and Hwang model (1985) Eq. 10	68.16	96.88	97.28	98.06	98.70

membrane, calculated permeance for CO₂ are in good agreement with experimental permeance having AARE % value of 0.66 %.

Evaluation of Existing Models using Polymeric blend Membrane

Fig 9 (a, b, c and d) represents the comparison between the existing models and the experimental data for PSU/PVAc blend membranes at different feed pressure. It was found that with the addition of PVAc with different composition 5-20 wt. % in PSU, the deviation had increased in theoretical permeance as compared to experimental permeance. Modified Cho empirical and Cho empirical models show the gaps increased of calculated gas permeance of CO₂ as compared to experimental permeance. The calculated permeance from Lee and Hwang model obtained is far from the experimental permeance as discussed in the previous section.

A comparative summary of the deviations between the models is listed in Table-3. When 5-20 wt. % of PVAc was blended in PSU; the AARE% increased from 0.66 % to 48.92 % in modified Cho empirical model. It was also observed that Cho empirical and Lee and Hwang model increased AARE % for CO₂ permeance as obtained in the modified Cho empirical model for all polymeric blend membranes. This deviation in theoretical permeance was due to the absence of the PVAc content in the blend membrane. The PVAc addition caused the model below predicted because the existing models were describing the transport of gases through single polymers. Hence, an additional parameter that account for the effect of blending need to be included in the modified Cho empirical model in order to be used for modeling the synthesis PBM.

Fig 10 portrays the order of the deviation based on the AARE% with increasing composition of PVAc in PSU matrix. It was found that AARE% deviation is in the increasing order as modified Cho empirical model < Cho empirical model < Lee and Hwang model. The results show that the modified Cho empirical model provided the least deviation from the other models.

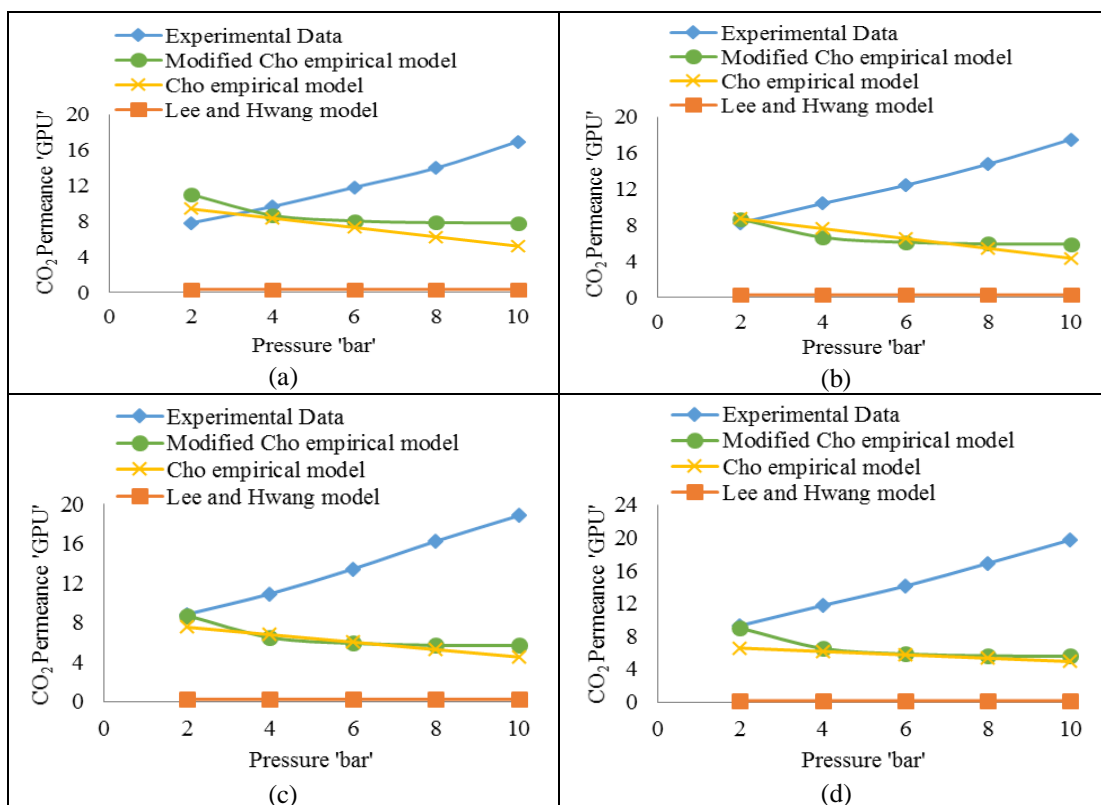


Fig. 9: Comparison of different models with experimental results for CO₂ permeance of (a) PSU/PVAc (95/5) wt. % (b) PSU/PVAc (90/10) wt. % (c) PSU/PVAc (85/15) wt. % (d) PSU/PVAc (80/20) wt. % polymeric blend membranes.

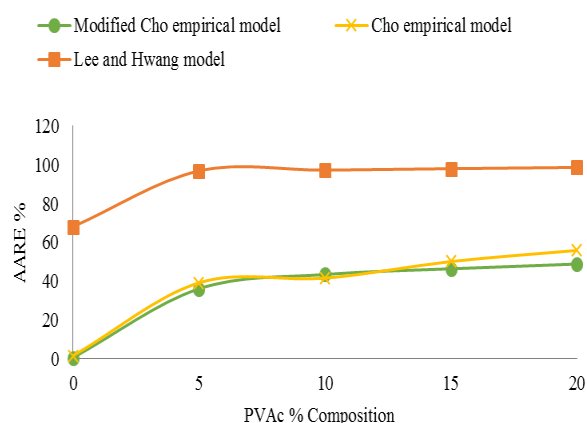


Fig. 10: Comparison of AARE% between existing models with increasing composition of PVAc in PSU for CO₂ permeance of polymeric blend membranes.

Evaluation of Existing Models using Enhanced Polymeric blend Membrane

Fig 11 (a, b, c and d) portrays the comparison between the existing models and the experimental data for PSU/PVAc/DEA enhanced polymeric blend membranes at 2 to 10 bar feed

pressure. It was found that with the addition DEA in PSU/PVAc blend membrane the deviation was further increased in theoretical permeance as compared to experimental permeance. This deviation shows the absence of DEA content in the enhanced polymeric blend membrane.

Table-4 shows the comparative summary of the deviations between the different models for PSU/PVAc/DEA enhanced polymeric blend membranes. However, the agreement between calculated permeance and experimental permeance for CO₂ changed when DEA 10 wt. % was added in a different composition of PSU/PVAc blend membrane; the AARE% also increased from 54.99 % to 73.40 % in modified Cho empirical model. This table also shows the comparison of calculated permeance and experimental permeance values of CO₂ using Cho empirical model and Lee and Hwang model. It was observed that the Cho empirical and Lee and Hwang model gave more error of calculated permeance with increased AARE% for CO₂ permeance. These might be due to the same reasons as stated for CO₂ permeance as the model fail to incorporate the effect of amine.

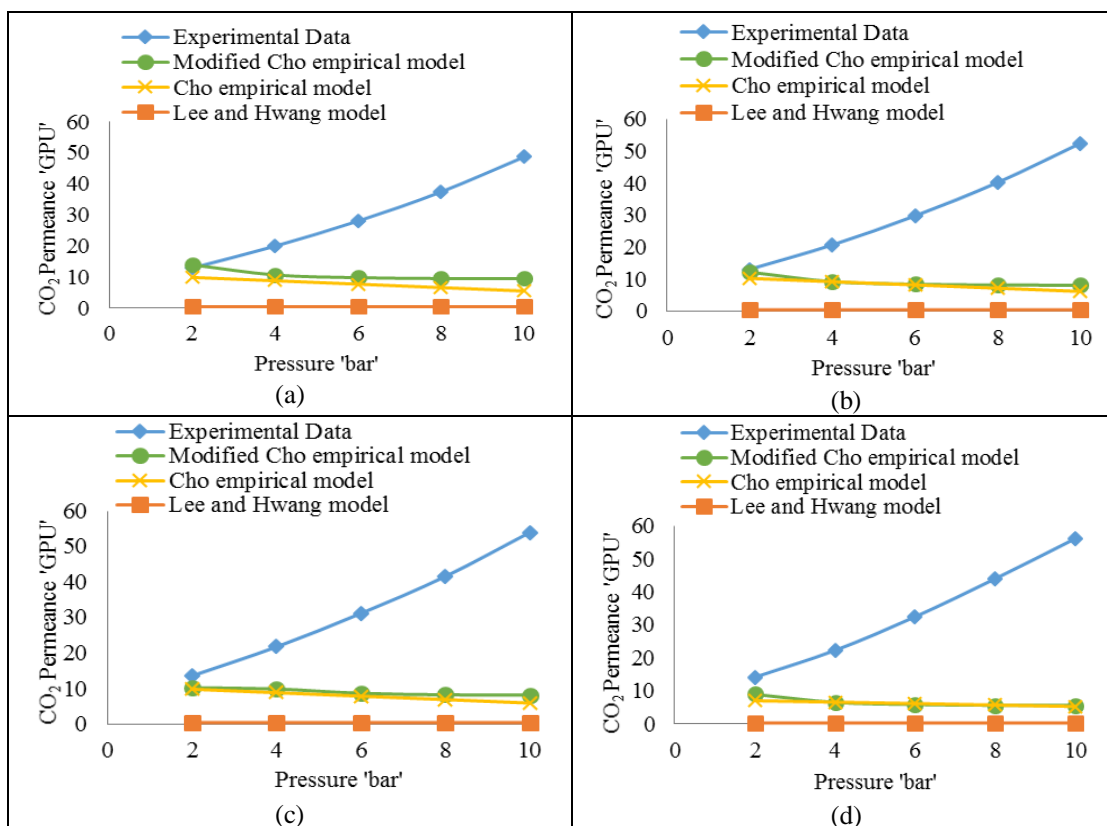


Fig. 11: Comparison of different models with experimental results for CO₂ permeance of (a) PSU/PVAc (95/5) wt. % /DEA (b) PSU/PVAc (90/10) wt. % /DEA (c) PSU/PVAc (85/15) wt. % /DEA (d) PSU/PVAc (80/20) wt. % /DEA enhanced polymeric blend membranes.

Table-4: Variation of the different existing models with the experimental data for CO₂ permeance of enhanced polymeric blend membranes

Theoretical models	Average Absolute Relative Error (AARE %) of enhanced polymeric blend membranes			
	PSU/PVAc (95/5) wt. % /DEA	PSU/PVAc (90/10) wt. % /DEA	PSU/PVAc (85/15) wt. % /DEA	PSU/PVAc (80/20) wt. % /DEA
Modified Cho empirical model (2004) Eq. 39	54.99	59.67	63.42	73.40
Cho Empirical model (1995) Eq. 30	64.06	64.73	66.97	75.98
Lee and Hwang model (1985) Eq. 10	97.31	98.53	98.67	99.19

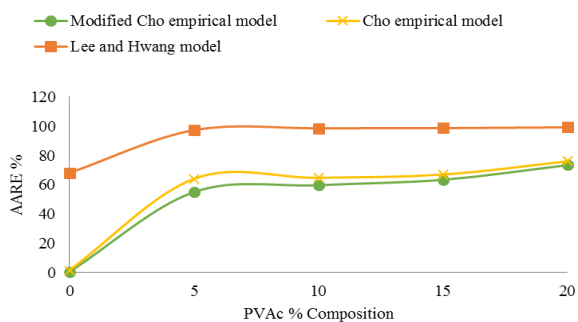


Fig. 12: Comparison of AARE% between existing models with increasing composition of PVAc in PSU with DEA for CO₂ permeance of enhanced polymeric blend membranes

Fig 12 shows the comparison of AARE% between existing models with increasing composition of PVAc in PSU with DEA of enhanced polymeric blend membranes. This Fig shows that the modified Cho empirical model provided the least deviation as compared to the other models. For CO₂ the AARE% between calculated permeance and experimental permeance was less at adding of PVAc content and high at adding of PVAc/DEA content as compared to base PSU membrane.

Selecting Suitable Model for Enhanced Polymeric Blend Membrane

The order of the deviation based on the AARE% equation (40) was found in the increasing order as modified Cho empirical model < Cho

empirical model < Lee and Hwang, respectively. The Lee and Hwang model represent only single phenomena (viscous diffusion). Thus this model did not predict whole phenomena's occurs in the porous membrane. The results show that the modified Cho empirical model provided the least deviation from the experimental data. This provides a rationale to use modified Cho empirical model as the base equation. However, significant deviations were observed between the calculated data from the theoretical models and the published experimental results which trigger a need for an improved model. Thus, the analysis on the range of the results obtained from the theoretical models seems to point towards the importance of morphology factors that need to be considered as well.

Observation from the FESEM cross-sectional view of the EPBM is described, indicates that the pores are uniform and a packed bed of spheres is a perfect sphere as assumed in the theoretical model. The blend (PVAc and amine) incorporate a spherical shape in the packed bed of

sphere [28, 35]. The assumptions are in good agreement with the morphology of membrane cross section. In order to account for the blend factor, modified Cho empirical model was used for the follow-up calculations.

There are some limitations with the theoretical equation as experimental values differ significantly with the theoretical values obtained from the equation (39) when PVAc and amines were blended in PSU. The experimental values have been repeated and re-evaluated to obtain reliability and assurance. Therefore, no significant change had been found with the experimental value. Since the main difference between EPBM and base membrane is caused by blending, a 'blending factor' can be introduced to incorporate the effects of blending in the EPBM.

Algorithm of Gas Permeance Modelling

To evaluate the gas permeance using the theoretical permeation models, experimental data was taken from CO₂ permeance in EPBM.

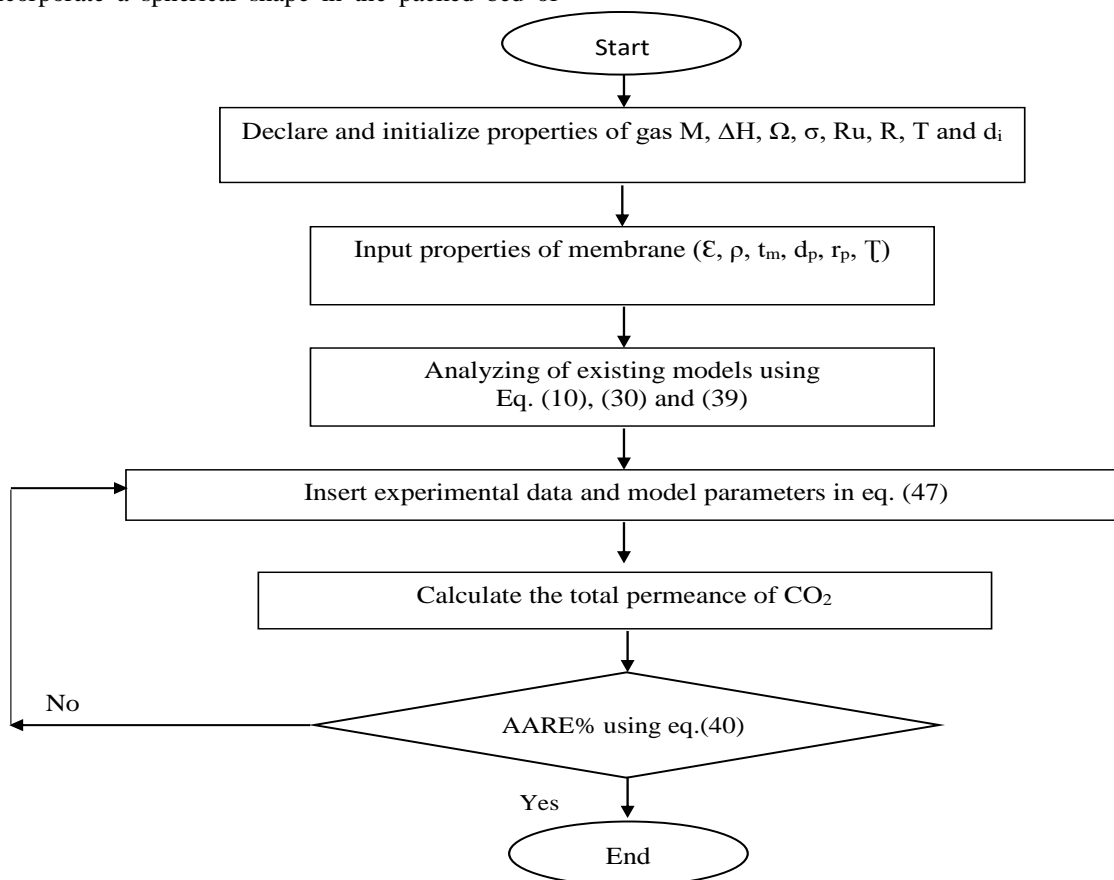


Fig 13: shows the detailed algorithm to solve the mathematical model for CO₂ permeance and selectivity. A combination of equations, text, and diagrams in an open screen environment made the application development easy.

Extended Modified Cho Empirical Model

As discussed, modified Cho empirical model was used as the base model in this study. The basic modified Cho empirical model equation (39) is chosen on the basis of some characteristics such as the summation of all three diffusion models (viscous, Knudsen and surface diffusions). It has simple formulation, incorporate all parameters of the porous membrane and less number of assumptions required to model the performance of EPBM. However, the model needs modifications in order to predict the permeance and selectivity of blended membranes. The permeance of a membrane depends on its plasticization and intrinsic absorptivity. When PSU blends with PVAc, enhances the permeance as PVAc chains contain polar carbonyl groups that can collaborate with CO₂ polar gas and increase the CO₂ solubility in the PSU/PVAc blend membranes. When the MDEA, DEA or MEA were added, they got incorporated into the pores of the membrane and thus increase the intrinsic absorptivity of the membrane. It was also observed that alkanolamine solution was embedded in the polymer matrix which offered the facilitated transport to CO₂ and retards the transport of CH₄. Assumptions are important for the models developed to be meaningful. Below are the few assumptions made in this modeling work;

- The membrane is assumed to be operated isothermally with in the feed and retentate side.
- The PVAc and DEA are homogenously distributed in the sphere of enhanced polymeric blend membrane.
- No reaction takes place in the membrane separation space available.
- No capillary condensation (multilayer adsorption) in the pores.
- Complete mixing occurs in both the feed and permeates chamber and that the bulk gas phase is moving in a plug flow manner.

When the pressure is increased, the effect is distributed between the blending material and the resulting pores. Small pore sizes provide narrow pathways of travel. Therefore the movement of the gas molecules is obstructed. Increasing operative pressure would increase the collision as well as the interaction between the gas molecules and membrane surface which makes surface diffusion more favourable. Surface diffusion increases primarily because of adsorption processes are favoured at high pressure due to increased molecular density. As a result, the tendency of filler material to absorb CO₂ as compared to CH₄ increases. It can be concluded that

the blending effect manifests itself as a strong function of pressure.

Estimation of PVAc factor in Blending factor

Modified Cho empirical model predicts the permeance of a porous membrane. When a polymer is blended, there is a significant change in its morphology and therefore, the deviation from experimental results is inevitable. Hence, an additional parameter that account for the effect of blending need to be included in the modified Cho empirical model in order to be used for modeling the synthesis PBM. Modelling can be done by considering PBM first, as it provokes the need of blending factor. To extend the basic modified Cho empirical model with the presence of the second component, PVAc an additional parameter is introduced which is the blend factor as a composition of 'x' of PVAc is introduced in equation (39).

This concept of adding a correction factor for improvement of prediction of parameters is not novel. In the case of the Virial equation of state, in which deviation of gas from ideal gas behaviour is predicted by defining a correction factor (named "compression factor") [36]. Another example from the equations for permeability prediction can be observed in Pal's model which can be obtained by adding a factor into the original Bruggmen's model [37].

To determine the blending factor theoretically is cumbersome. Nevertheless, the blending factor could be determined through data fitting and optimization of predicted parameters against experimental data to minimize the model prediction errors. Defining the blending factor as:

$$\text{Blend factor } (B_{f,p,cal}) = 1 + \sum_{i=1}^3 a_i x^i \quad (41)$$

or

$$\text{Blend factor } (B_{f,p,cal}) = 1 + a_1 x + a_2 x^2 + a_3 x^3 \quad (42)$$

The blend composition 'x' represents the fraction of PVAc in this study. Its value varies between 0 and 1, where 0 represents the pure polymer. The parameter a_1, a_2, a_3 are function of pressure 'P', defined as:

$$a_i = f_i(P) = \alpha_i + \beta_i P + \gamma_i P^2 + \theta_i P^3 + \phi_i P^4 \quad (43)$$

where; P is the pressure, α , β , γ , θ and ϕ are blending constants.

The blend factor is included into the equation (39) to obtain precise theoretical values that are close to the experimental values. The new extended modified Cho empirical model equation to address the deviation will provide an accurate estimation of the theoretical values.

$P'_i = \text{Base equation} \times \text{Blending factor of PVAc}$

$$P'_i = \left[\frac{\epsilon r_p^2 P}{8\tau\mu_i zRT} + \frac{\epsilon}{z\tau RT} \left\{ \left(\frac{1}{D_i} + \frac{1}{D_{k,i}} \right) + 2 \frac{t_m \epsilon}{r_p \tau} (1 - \epsilon) (\mathcal{O}_s \rho_m f) \right\} \right] \times \left[1 + \sum_{i=1}^3 a_i x^i \right] \quad (44)$$

The calculated $B_{f,p,cal}$ was determined by using equation (42). On the other hand, the experimental values of the blending factor $B_{f,exp}$ can be determined using the following expression:

$$B_{f,exp} = \frac{P'_i (\text{exp})}{\left[\frac{\epsilon r_p^2 P}{8\tau\mu_i zRT} + \frac{\epsilon}{z\tau RT} \left\{ \left(\frac{1}{D_i} + \frac{1}{D_{k,i}} \right) + 2 \frac{t_m \epsilon}{r_p \tau} (1 - \epsilon) (\mathcal{O}_s \rho_m f) \right\} \right]} \quad (45)$$

The values of the model parameter constants, α , β , γ , θ and ϕ for a_1 , a_2 and a_3 can be found from Table-5. This table shows the optimized blending parameter constant from the fitting process when PVAc was added in the PSU matrix. At this optimized $B_{f,p,cal}$, all the parameters contact should satisfy all fitted experimental conditions and reach at a unique solutions. In order to find the values which can provide sufficient approximation of the blending factor $B_{f,p,cal}$, the MATLAB® curve-fitting tool was used for selecting initial guesses of these values. It should be noted that to avoid overfitting, only low order equations were used in accordance with the trends of the experimentally observed values of the blending factor for compositions PSU/PVAc (80/20) wt. %, PSU/PVAc (90/10) wt. % and PSU/PVAc (95/5) wt. %. Thus the parameter constants were optimized at which the calculated blending factor $B_{f,p,cal}$, for these compositions would approach the experimental blending factor $B_{f,exp}$.

Table-5: Blending factor parameters for PSU/PVAc blends.

Blend Parameter Constants	α	β	γ	θ	ϕ
a_1	-29.202	11.653	-1.3156	0.0725	0
a_2	288.6	-104.96	15.619	-0.9005	0
a_3	-823.56	296.61	-48.424	2.8094	0

Table-6: Calculated and experimental values of blending factor for CO₂ permeance at different pressures of polymeric blend membranes

Membranes	Pressure 'bar'	"B _f " for CO ₂ permeance		
		$B_{f,exp}$	$B_{f,p,cal}$	AARE%
PSU/PVAc (95/5) wt. %	2	0.7085	0.76	
	4	1.1127	1.17	
	6	1.4691	1.49	3.11
	8	1.7802	1.80	
	10	2.1663	2.18	
PSU/PVAc (90/10) wt. %	2	0.949	0.880	
	4	1.563	1.478	
	6	2.029	1.987	3.23
	8	2.482	2.458	
	10	2.953	2.940	
PSU/PVAc (80/20) wt. %	2	1.0326	1.029	
	4	1.8013	1.785	
	6	2.4140	2.425	0.42
	8	3.0023	2.997	
	10	3.5377	3.546	

Subsequently, using optimized blending parameters, the calculated blending factor $B_{f,p,cal}$, was determined using equation (42). The comparison between $B_{f,exp}$, calculated using equations (45) and (42) are tabulated in Table-6. The AARE% for all conditions fit very well with less than 3%.

The experimental data of composition PSU/PVAc (85/15) wt. % has been with-held for cross-validation of the resulting model in order to avoid overfitting. To validate these blending constants, a new set of experimental data was used at PSU/PVAc (85/15) wt. %. The results are presented in Table-9 with AARE% < 2%. The blending factors $B_{f,p,cal}$, are then multiplied in equation (39) when PVAc is blended in PSU to normalize the surface diffusion, Knudsen diffusion and viscous diffusion in total permeance using modeling from 2 to 10 bar pressure.

Estimation of amine factor in Blending factor

In order to extend the basic modified Cho empirical model with the presence of the third component that is an amine, an additional parameter is introduced which is the combined blend factor as a composition of 'y' of amine is introduced in equation (41) as:

$$\text{Blend factor } (B_{f,pa,cal}) = 1 + \sum_{i=1}^3 a_i x^i + \sum_{i=4}^6 a_i y^{i-3} + \sum_{i=7}^8 a_i x^{i-6} y^{9-i} \quad (46)$$

or

$$B_{f,pa,cal} = 1 + a_1 x + a_2 x^2 + a_3 x^3 + a_4 y + a_5 y^2 + a_6 y^3 + a_7 x y^2 + a_8 x^2 y \quad (47)$$

The amine composition y represents the fraction of amine in the membrane. Its value varies between 0 and 1, where 0 represents the absence of

amine. The parameter a_i a function of pressure P , defined as:

$$a_i = f_i(P) = \alpha_i + \beta_i P + \gamma_i P^2 + \theta_i P^3 + \phi_i P^4 \quad (48)$$

where P is the pressure, α , β , γ , θ and ϕ are blending constants.

The blend factor is included into the equation (39) to obtain precise theoretical values that are close to the experimental values. The extended modified Cho empirical equation to evaluate the error percentage that will provide an accurate estimation of the theoretical values is as follows:

$$P'_i = \text{Base equation} \times \text{Blending factor of PVAc and amine}$$

$$P'_i = \left[\frac{C_{T_1} P^2}{8T_{10} RT} + \frac{C}{T_1 RT} \left(\frac{1}{D_1} + \frac{1}{D_{2,1}} \right) + 2 \frac{t_m E}{P^2} (1 - \epsilon) (D_2 \rho_m P) \right] \times \left[1 + \sum_{i=1}^3 a_i x^i + \sum_{i=4}^6 a_i y^{i-2} + \sum_{i=7}^8 a_i x^{i-6} y^{9-i} \right]$$

The values of α , β , γ , θ and ϕ for a_1, a_2, \dots, a_8 can be found from Table-7. It should be noted that the values of a_1, a_2 and a_3 were previously determined. Hence, only the values of a_4, a_5, \dots, a_8 are now obtained by minimizing the prediction error of compositions PSU/PVAc (80/20) wt. % /DEA, PSU/PVAc (90/10) wt. % /DEA and PSU/PVAc (95/5) wt. % /DEA. MATLAB® curve-fitting tool was used for selecting appropriate initial guesses, whereas fine-tuning of the parameter was obtained by hit-and-trial in a spreadsheet, as was previously done for the determination of a_1, a_2 and a_3 in above section.

Table-7: Blending factor parameters for PSU/PVAc/DEA.

Blend Parameter Constants	α	β	γ	θ	ϕ
a_1	-29.202	11.653	-1.3156	0.0725	-
a_2	288.6	-104.96	15.619	-0.9005	-
a_3	-823.56	296.61	-48.424	2.8094	-
a_4	-0.253	0.237	-0.072	0.009	-
a_5	-1144.9	1060.9	-315.72	39.64	-1.72
a_6	0.01	-0.04	-0.03	-0.004	-
a_7	1224.3	-471.23	-69.893	5.745	-
a_8	-155.41	-25.77	87.396	-5.8892	-

The calculated $B_{f,pa,cal}$ was intended by using equation (46), whereas the experimental $B_{f,exp}$ was determined by using equation (45). The calculated and experimental values of the blending factor for different blending compositions and pressures are shown in Table-8. The AARE% for all conditions fit very well with less than 8%.

Table-8: Blending Calculated and experimental values of blending factor for CO₂ permeance at

different pressures of enhanced polymeric blend membranes.

Membranes	Pressure 'bar'	"B _f " for CO ₂ permeance		
		$B_{f,exp}$	$B_{f,pa,cal}$	AARE%
PSU/PVAc (95/5) wt. % /DEA	2	0.9262	0.840	
	4	1.8729	2.108	
	6	2.8694	2.373	8.96
	8	3.9459	4.345	
	10	5.1547	5.126	
PSU/PVAc (90/10) wt. % /DEA	2	1.0725	1.060	
	4	2.2478	2.279	
	6	3.5448	3.600	5.56
	8	4.9388	4.625	
	10	6.4745	5.351	
PSU/PVAc (80/20) wt. % /DEA	2	1.5810	1.545	
	4	3.4289	3.463	
	6	5.5718	5.852	3.07
	8	7.8499	7.736	
	10	10.101	9.535	

As in the previous section, the experimental data of composition PSU/PVAc (85/15) wt. % /DEA has been withheld for cross-validation of the resulting model to avoid overfitting. To validate these blending constants, a new set of experimental data was used at PSU/PVAc (85/15) wt.% /DEA. The results are presented in Table 9 with AARE% < 3%. The blending factors $B_{f,pa,cal}$ are then multiplied in equation (39) to normalize, when PVAc and amine are blended in PSU from 2 to 10 bar pressure.

Comparison of Extended Modified Cho Empirical Model and Experimental Blending Factor of Polymeric Blend Membrane and Enhanced Polymeric Blend Membrane

The experimental and calculated blending factor for CO₂ permeance was compared on the basis of the composition blend of PSU/PVAc (85/15) wt. % and PSU/PVAc (85/15) wt. % /DEA as shown in Table 9.

Table-9: Validation of experimental values with blending factor for CO₂ permeance of PSU/PVAc (85/15) wt. % and PSU/PVAc (85/15) wt. % /DEA at different pressure.

Membranes	Pressure 'bar'	"B _f " for CO ₂ permeance		
		Experimental	Calculated	AARE%
PSU/PVAc (85/15) wt. %	2	1.017	1.072	
	4	1.688	1.739	
	6	2.295	2.342	2.29
	8	2.872	2.884	
	10	3.349	3.368	
PSU/PVAc (85/15) wt. % /DEA	2	1.329	1.395	
	4	2.283	2.388	
	6	3.616	3.471	3.76
	8	5.069	5.182	
	10	6.660	6.459	

Fig 14 shows the plot from the results for PSU/PVAc (85/15) wt. % and PSU/PVAc (85/15) wt. % /DEA blend membrane for calculated and experimental blending factor. This Fig shows the comparison of calculated blending factor of CO₂

permeance using the extended modified Cho empirical model with experimental data. As expected, an excellent agreement between the calculated and experimental data for PSU/PVAc (85/15) wt. % and PSU/PVAc (85/15) wt. % /DEA blend membrane, all points meet at 45° slope.

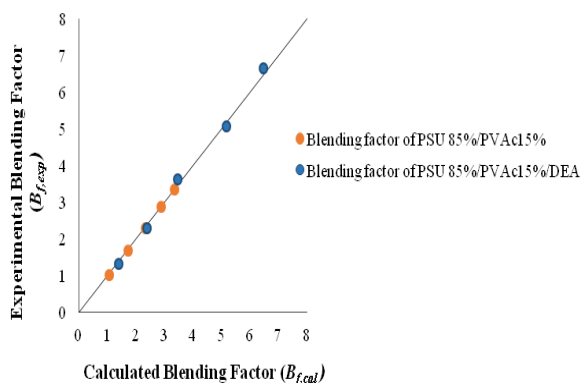


Fig. 14: Comparison between calculated and experimental blending factor for PSU/PVAc (85/15) wt. % and PSU/PVAc (85/15) wt. % /DEA for CO₂ permeance.

Mechanism of Gas Molecules Flow in EPBM

Fig. 15 shows the CO₂ permeance calculated using the extended modified Cho empirical model (incorporate of blending factor) compared with the experimental data. As can be seen from Fig 15, surface diffusion is the dominant contributor to the total permeance of CO₂ at small pores and it decreases with increasing pore size. This is in accordance with the theory as suggested by Hsieh [30].

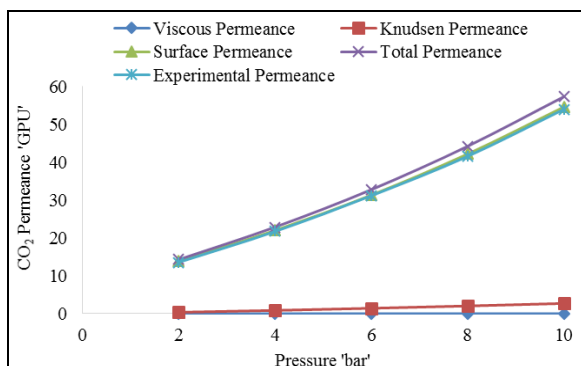


Fig. 15: Comparison of theoretical and experimental data of PSU/PVAc (85/15) wt. % /DEA membrane in terms of CO₂ permeance.

Due to the hindered paths of travel, viscous diffusion and Knudsen diffusion are not apparent at small pore sizes. The effects are clearly visualized at pore size less than 2 nm. At higher pore size, Knudsen diffusion becomes more apparent and contributes the most to the total permeability of pure CO₂ molecules across the membrane [12, 16]. The CO₂ molecules would now collide more frequently with the pore walls rather than colliding with the neighbouring CO₂ molecules (viscous diffusion) [12, 14, 21]. This is again in accordance with the theory as obtained from Burggraaf and Cot as well as modeling work by Othman [18].

This Fig also shows that permeance of CO₂ increases with increasing operating pressure. As discussed above, surface diffusion predominates Knudsen and viscous diffusion at small pore regions. This circumstance occurs as a result of strong surface diffusion mechanism. Increasing operative pressure would increase the collision as well as the interaction between the gas molecules and membrane surface which make surface diffusion more favourable. Surface diffusion increases in this case primarily because of adsorption processes are favoured at high pressure due to the increased molecular density of the gas components. On the other hand, Knudsen diffusion is not sensitive at all to operating pressure. The increments possibly caused by one of its physical properties that are called compressibility factor z .

Table-10: Average absolute relative error percent between experimental and modeling data for different polymeric blend membranes and enhanced polymeric blend membranes

Membranes	Average Absolute Relative Error (AARE %) CO ₂ Permeance
PSU/PVAc (95/5) wt. %	3.12
PSU/PVAc (90/10) wt. %	3.24
PSU/PVAc (85/15) wt. %	2.28
PSU/PVAc (80/20) wt. %	0.41
PSU/PVAc (95/5) wt. % /DEA	5.13
PSU/PVAc (90/10) wt. % /DEA	4.67
PSU/PVAc (85/15) wt. % /DEA	5.17
PSU/PVAc (80/20) wt. % /DEA	4.92

The deviation obtained between the predicted and the experimental values were calculated using the percentage average absolute relative error (AARE%) as depicted by the equation (40). The errors are calculated as an average error from 2 to 10 bar. The results show that the developed model is quite accurate and reliable with the average absolute relative deviation as shown in Table 10. The values of AARE% was found in the range of 0.5 to 3.50%

and 4.5 to 5.5% for all pressure range of polymeric blend membrane and enhanced polymeric blend membrane, respectively. AARE% values confirm that the relative deviation of the developed model from the experimental data is almost negligible.

Comparison of Existing and Proposed Models with Experimental Results

Fig 16 shows the comparison of experimental results with a proposed model in the literature for CO₂ permeance at different feed pressures. The proposed model is plotted to compare its predictions against the experimental results and previous models.

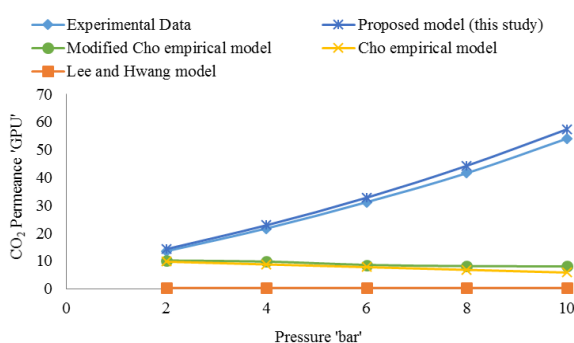


Fig. 16: Comparison between existing and proposed model with experimental results of CO₂ permeance for PSU/PVAc (85/15) wt. % /DEA.

From the Fig, it is clear that the extended modified Cho empirical model proposed in this study can predict the gas permeance and selectivity with reasonable accuracy, whereas the previous models fail to take account of the effects of blending. The results show that the proposed model is quite accurate and reliable in forecasting the gas permeance and selectivity of blended membranes of different compositions due to the incorporation of blending factor.

Conclusion

The comparison between theoretical modeling and experimental data regarding the principal mechanisms of gas permeation in porous material consist of viscous diffusion, Knudsen diffusion, and surface diffusion is evaluated. There is a limitation within the modified Cho. Empirical model equation and therefore, requires another parameter to be included. In practice, the blending factors are calculated to multiply in the equation when PVAc and amines are blended in PSU to

normalize the surface diffusion, Knudsen diffusion and viscous diffusion in total permeance using modeling from 2 to 10 bar pressure. In EPBM the pore surface, adsorption of CO₂ gas molecules (strongly adsorbing gas) takes place and thus, contributes to the high total permeability of CO₂. Due to the hindered paths of travel, viscous diffusion and Knudsen diffusion are not apparent at small pore sizes. The effects are clearly visualized at pore size less than 1 nm. The permeability of CO₂ increases with increasing operating pressure. As surface diffusion predominates Knudsen and viscous diffusion at small pore regions. This circumstance occurs as a result of strong surface diffusion mechanism. This suggests that the EPBM membrane, as the one used in this study, should be manufactured to have a pore size less than 1 nm for it to be economic and selective for CO₂ removal from CH₄. The results show that the developed model is quite accurate and also reliable with the average absolute relative deviation. The mathematical model developed in this study can predict the actual scenario of gas permeation reasonably all points are meet at 45° slope. However, there are still many more studies that can be extended from this endeavor to improve the models developed at a relatively low temperature and high pressure, some gases will undergo capillary condensation (multilayer adsorption), when the adsorbed molecules form layers on top of each other and eventually condense and clog the pores of the membrane. It is strongly recommended that the effect of capillary condensation could be taken into account for future studies, as it plays an important role under certain operating conditions.

Acknowledgement

The authors would like to acknowledge the Universiti Teknologi PETRONAS, Malaysia for supporting this research work and the NED University of Engineering & Technology, Karachi, Pakistan for financial support to Asim Mushtaq, studying at this University.

Nomenclature			
CO ₂	Carbon dioxide	EPBM	Enhanced Polymeric Blend Membranes
CH ₄	Methane	PSU	Polysulfone
DEA	Diethanolamine	PVAc	Polyvinyl acetate

LIST OF SYMBOLS

Symbol	Definition	Units
A_m	Area of the membrane.	[m ²]
$B_{f,p,cal}$	Blending factor of polymer calculated	[-]
$B_{f,pa,cal}$	Blending factor of polymer amine calculated	[-]
$B_{f,exp}$	Blending factor of experimental	[-]
C_g	Concentration of gas	[mol.L ⁻¹]

C_s	Concentration of gas molecules adsorbed onto the surface	[mol.L ⁻¹]
v	Velocity of gas	[m.s ⁻¹]
d_i	Diameter of gas molecule i	[m]
d_p	Membrane pore diameter	[m]
D_b	Bulk diffusivity	[cm ² .s ⁻¹]
D_{ei}	Effective diffusivity of gas i	[cm ² .s ⁻¹]
D_i	Ordinary gas diffusivity for i	[cm ² .s ⁻¹]
$D_{i,mix}$	Ordinary diffusivity of gas in a mixture	[m ² .s ⁻¹]
D_{Ki}	Knudsen diffusivity for i	[cm ² .s ⁻¹]
D_s	Surface diffusivity	[cm ² .s ⁻¹]
D_v	Viscous diffusivity	[cm ² .s ⁻¹]
db/dp	Wall to wall pore distance	[m]
f	Equilibrium loading factor	[m ³ .kg ⁻¹]
ΔH	Heat of vaporization	[J.mol ⁻¹]
J_T	Total effective flux of the gas molecules	[mol.m ⁻² .s ⁻¹]
L_m	Length of the cylindrical pore	[m]
M_i	Molecular weight of gas i	[kg.kmol ⁻¹]
M_j	Molecular weight of gas j	[kg.kmol ⁻¹]
\bar{P}	Average pressure across the membrane	[atm]
P'_i	Permeability of gas i	[mol.s.kg ⁻¹]
P_k	Knudsen permeability	[mol.s ⁻¹][m][m ²][kg ⁻¹ .m.s]
P_r	Ratio of permeate pressure divided by the feed pressure	[-]
p_h	High-pressure side	[atm]
p_l	Low-pressure side	[atm]
ΔP	Pressure drop across the membrane	[atm]
P_s	Surface permeability	[mol.s ⁻¹][m][m ²][kg ⁻¹ .m.s]
P_v	Viscous permeability	[mol.s ⁻¹][m][m ²][kg ⁻¹ .m.s]
q_A	Flow rate of A in permeate	[cm ³ (STP).s ⁻¹]
q_f	Total feed flow rate	[cm ³ (STP).s ⁻¹]
q_o	Outlet reject flow rate	[cm ³ (STP).s ⁻¹]
q_p	Permeate flow	[mol.s ⁻¹]
R	Universal gas constant	[82.06 cm ³ .atm.mol ⁻¹ .K ⁻¹]
R_m	Radius of cylindrical pore	[m]
r_p	Pore radius	[m]
T	Temperature	[K]
t_m	Membrane thickness	[m]
v	Structural volume increment	[m ³]
x_o	Reject mole fraction	[-]
y	Mole fraction at the permeate side	[-]
y_p	Permeate mole fraction	[-]
z	Compressibility factor	[-]
\mathcal{E}	Membrane porosity	[-]
μ_i	Viscosity of gas i	[kg.m ⁻¹ .s ⁻¹]
$\mu_{i,mix}$	Average viscosity for the gas mixture	[kg.m ⁻¹ .s ⁻¹]
η	Shape factor of the membrane	[-]
λ	Mean free path of travel of gas molecules in the pore	[m]
τ	Membrane tortuosity	[-]
ρ_m	Membrane density	[kg.m ⁻³]
Ω_μ	Lennard-Jones parameters as available in Bird et al.(1960)	[-]
σ	Kinetic diameter of gas molecule	[°A]

References

- C. A. Scholes, G. W. Stevens and S. E. Kentish, Membrane gas separation applications in natural gas processing, *Fuel*, **96**, 15 (2012).
- M. Mulder, Basic principles of membrane technology, *Springer Sci. Bus. Media*, 12 (1996).
- M. W. Uddin, and May-Britt Hägg, Natural gas sweetening the effect on CO₂/CH₄ separation after exposing a facilitated transport membrane to hydrogen sulfide and higher hydrocarbons, *J. Membr. Sci.*, **423**, 143 (2012).
- O. Vopička et al., Equilibrium and transient sorption of vapours and gases in the polymer of intrinsic microporosity PIM-1, *J. Membr. Sci.*, **434**, 148 (2013).
- H. J. Kim, and Suk-In Hong, The sorption and permeation of CO₂ and CH₄ for dimethylated polysulfone membrane, *Korean J. Chem. Eng.*, **14**, 168 (1997).
- J. G. S. M. and, T. T. Tsotsis. (Wiley-vch, 2001), pp. 1-10.
- E. J. Henley, Junior D. Seader, and D. Keith Roper, Separation process principles, *wiley*, 86 (2011).
- R. W. Baker, K. Lokhandwala, Natural gas processing with membranes: an overview, *Ind. Eng. Chem. Res.*, **47**, 2109 (2008).
- R. E. Cunningham, and R. J. J. Williams, Diffusion in gases and porous media, *New York: Plenum press*, 145 (1980).
- A. J. Burggraaf, and Louis Cot, Fundamentals of inorganic membrane science and technology, *Elsevier*, **4**, 25 (1996).
- K. Scott, Membrane separation technology, *Scientific & Technical Information*, 32 (1990).
- R. W. Baker, *Membrane Technology and Applications: Overview of membrane science and technology*. (Wiley, New York, ed. 3, 2012), vol. 3rd, pp. 1-14.
- N. N. Li, Anthony G. Fane, WS Winston Ho, and Takeshi Matsuura, eds, Advanced membrane technology and applications, *John Wiley & Sons*, 22 (2011).
- K.-H. Lee, and Sun-Tak Hwang, The transport of condensable vapors through a microporous Vycor glass membrane, *J. Colloid Interface Sci.*, **110**, 544 (1986).
- R. B. Bird, Transport phenomena, *Appl. Mech. Rev.*, **2**, 25 (2002).
- G. George, N. Bhoria, S. AlHallaq, A. Abdala, V. Mittal, Polymer membranes for acid gas removal from natural gas, *Sep. Purif. Technol.*, **158**, 333 (2016).
- R. J. R. Uhlhorn, K. Keizer, and A. J. Burggraaf, Gas and surface diffusion in modified γ -alumina systems, *J. Membr. Sci.*, **46**, 225 (1989).
- L. C. Han, Study of Gas Permeability and Separation Behaviour for Removal of High Content CO₂ from CH₄ by Using Membrane Modelling, *Thesis, Universiti Teknologi Petronas* (2004).
- K. Keizer, R. J. R. Uhlhorn, and A. J. Burggraaf, Gas separation mechanisms in microporous modified γ -Al₂O₃ membranes, *J. Membr. Sci.*, **39**, 285 (1988).
- R. M. Felder, and Ronald W. Rousseau, Elementary principles of chemical processes, *Wiley*, 381 (2005).

21. Y.-K. Cho, Kunwoo Han, and Kun-Hong Lee, Separation of CO₂ by modified γ -Al₂O₃ membranes at high temperature, *J. Membr. Sci.*, **104**, 219 (1995).
22. J. E. Koresch, A. Soffer, The Carbon Molecular Sieve Membranes. General Properties and the Permeability of CH₄/H₂Mixture, *Sep. Sci. Technol.*, **22**, 973 (1987).
23. S. Kim, Y. M. Lee, Rigid and microporous polymers for gas separation membranes, *Prog. Polym. Sci.*, **43**, 1 (2015).
24. H. M. a. L. C. Han, Permeability Studies of Carbon Dioxide and Methane across γ -Alumina Membrane, *Proceedings of the 18th Symposium of Malaysian Chemical Engineers*, **2**, 101 (2004).
25. J. A. H. Dreyer et al., Simulation of gas diffusion in highly porous nanostructures by direct simulation Monte Carlo, *Chem. Eng. Sci.*, **105**, 69 (2014).
26. M. Hedenqvist, and U. W. Gedde, Diffusion of small-molecule penetrants in semicrystalline polymers, *Prog. Polym. Sci.*, **21**, 299 (1996).
27. A. Mushtaq, H. Mukhtar, A. M. Shariff, Gas Permeability and Selectivity of Synthesized Diethanol Amine-Polysulfone/Polyvinylacetate Blend Membranes, *Res. J. Appl. Sci. Eng. Tech.*, **8**, 600 (2014).
28. A. Mushtaq, H. Mukhtar, A. M. Shariff, Advanced Development and Characterization of DEA Amine-Polysulfone/Polyvinylacetate Blend Membranes, *Res. J. Appl. Sci. Eng. Tech.*, **8**, 1201 (2014).
29. W. J. Koros, and Rajiv Mahajan, Pushing the limits on possibilities for large scale gas separation: which strategies, *J. Membr. Sci.*, **175**, 181 (2000).
30. H. P. Hsieh, Inorganic membranes for separation and reaction, *Elsevier*, **37** (1996).
31. H. Mukhtar, N. M. Noor, R. Nasir, D. F. Mohshim, Pore Model Prediction of CH₄ Separation from H₂S using PTMSP and γ - Alumina Membranes, *Int. J. Mater. Metall. Eng.*, **6**, 895 (2012).
32. M. R. Othman, H. Mukhtar, A. L. Ahmad, Gas permeation characteristics across Nano-porous inorganic membranes, *IJUM Eng. J.*, **5**, 17 (2004).
33. C. W. A. I. B. C. W. Azmi, Modeling of Carbon Dioxide and Nitrogen Removal From Natural Gas Using Membrane Processes, *Thesis, Universiti Teknologi Petronas* 1(2005).
34. G. Murshid, A. M. Shariff, L. K. Keong, M. A. Bustam, Physical Properties of Aqueous Solutions of Piperazine and (2-Amino-2-methyl-1-propanol + Piperazine) from (298.15 to 333.15) K, *J. Chem. Eng. Data*, **56**, 2660 (2011).
35. A. Mushtaq, H. Mukhtar, A. M. Shariff, Fabrication and Characterization of Synthesized Polysulfone/Polyvinylacetate Blend Membranes, *Res. J. Appl. Sci. Eng. Tech.*, **7**, 3094 (2014).
36. G. Halder, Introduction to chemical engineering thermodynamics, *PHI Learning* (2014).
37. B. Shimekit, H. Mukhtar, T. Murugesan, Prediction of the relative permeability of gases in mixed matrix membranes, *J. Membr. Sci.*, **373**, 152 (2011).